Supplementary information for dynamics of molten pool evolution and high-speed real-time optical measurement in laser polishing

S1 simulation principle

To analyze the accuracy of optical time-stretch imaging and to simulate the process of laser single-point heating of fused silica. The following assumptions were used to develop mathematical models of the heating, flow, and evaporation processes using finite element analysis software[1].

(1) It is assumed that the material is isotropic and homogeneous.

(2) Weakly compressible laminar flow.

(3) Ionization of the evaporating material and laser shielding are not taken into account.

The absorptivity of the material remains the main input assumption in the modelling and is a difficult quantity to measure, so a calibrated constant value is used[2].

The simulation ignores the shielding effect of the vapor plume on the laser, i.e., the proportion of the total energy absorbed by the material at different laser power densities, which is one of the reasons for the difference between the simulation and experimental results. In Figure 4 in the main text, as well as in the supplementary information figure s4, the density variation of the material is ignored in order to facilitate the calculation of ablation as well as the variation of roughness during polishing.

1. The implementation details of simulation procedures:

Figure s1 depicts the boundary conditions, and Table s1 contains the corresponding equations.

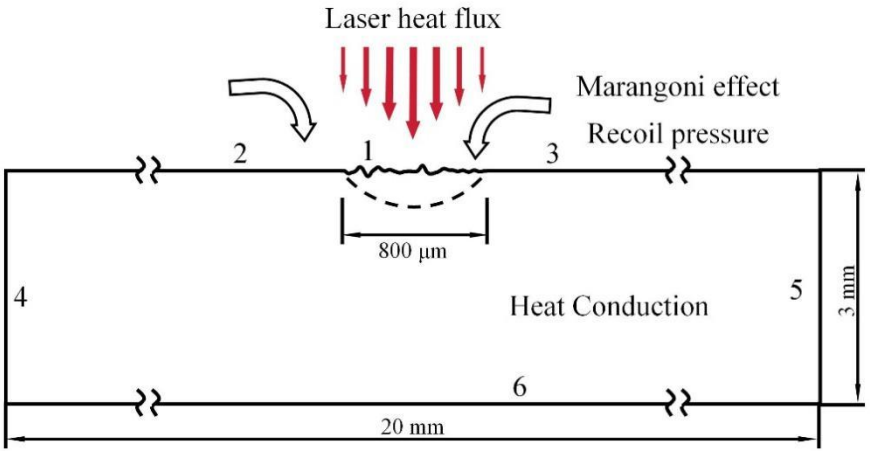

Figure s1. Schematic of the computation model

Table s1 governing equations and boundary conditions.[3]

Model	Boundary No.	Boundary Condition	Equation
Heat transfer model	Region		$\rho C_p\left[\frac{\partial T}{\partial t}+\nabla\cdot(\vec{V}T)\right]-\nabla\cdot(k\nabla T)=Q$
	1,2,3	Laser heat flux	$k\frac{\partial T}{\partial n}\Big\vert_{1,2,3}=Q-u_s\rho L_{ev}-h(T-T_{ext})-\varepsilon\cdot\sigma(T^4-T_{ext}^4)$
	1,2,3	Heat flux, evaporation, convection and radiation	$Q=I_0\exp\left(-\frac{2r^2}{r_0^2}\right)$
	4,5,6	Nature convection	$k\frac{\partial T}{\partial n}\Big\vert_{4,5,6}=-h_c(T-T_{ext})$
Fluid flow model	Region		$\rho\left(\frac{\partial \vec{V}}{\partial t}+\nabla\cdot(\vec{V}\vec{V})\right)+\mu\nabla^2\vec{V}+\nabla p=0$
	1,2,3	Marangoni effect	$\vec{\sigma}=\frac{\partial\gamma}{\partial T}\frac{\partial T}{\partial\vec{\tau}}\vec{\tau}$
	1,2,3	Recoil pressure	$P_{\text{recoil}}=\rho_v u_{\text{out}}^2$
Deformed geometry	4,5,6	Fixed boundary	$u=0$
	1,2,3	Deformation of melt flow	$u=\vec{n}\cdot\vec{V}+u_s$
	1,2,3	Ablation rate	$u=-\vec{n}\cdot\vec{V}-u_s$

The solid and fluid heat transfer model is strongly coupled with the laminar model, and the related coupled physical field is the Marangoni effect. The deformation geometry represents the change of material shape during the heating process.

Where $\vec{V}$ is the velocity of material, resulting from the evaporation and the flow of melt material, and ρ, μ, C_p and k are the density, viscosity, specific heat capacity, and heat conductivity in the simulations of fused silica. Where I_0 is the laser heat fluence, r_0 is the spot radius. Where u_s is the vaporization rate of target, L_{ev} is the latent heat of vaporization, and T_{ext} is the environment temperature.

Laser polishing parameters and constants used for simulation are listed in Table s2.

Table s2. Polishing parameters and constants

Parameter(unit)	Nomenclature	Value
Beam radius (μm)	r_c	650
Ambient temperature (K)	T_a	293.15
Initial temperature (K)	T_i	293.15
Convective coefficient (W / m^2 · K)	h_c	100
Stefan-Boltzmann constant (W / (m^2 · K^4))	σ	5.67×10^{-8}
Radiation emissivity	ε	0.91

S2. Material Properties

The transition point temperature of fused silica is 2273 K, and the evaporation temperature is 2973 K[4]. According to data from [5], Fig. s2(a) shows the density, heat capacity, and heat conductivity of fused silica as a function of temperature. Figure s2 (b). For fused silica, the viscosity in relation to temperature is shown [6]. The Vogel-Fulcher-Tamman equation is used to calculate the curves, and the data for the materials' viscosities are taken from their data sheets.

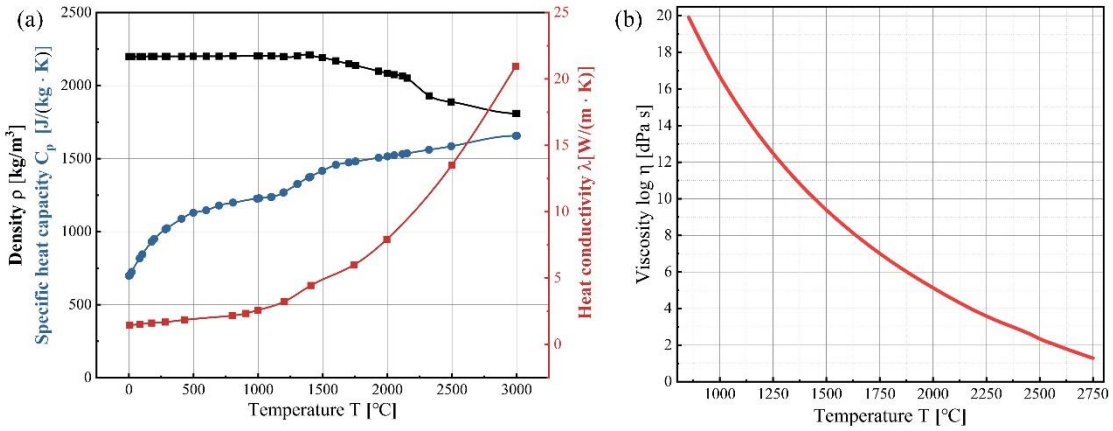

Figure s2. (a)Variation of density, heat conductivity, constant pressure heat capacity with temperature. (b)Variation of dynamic viscosity with temperature.

S3. Simulation Results

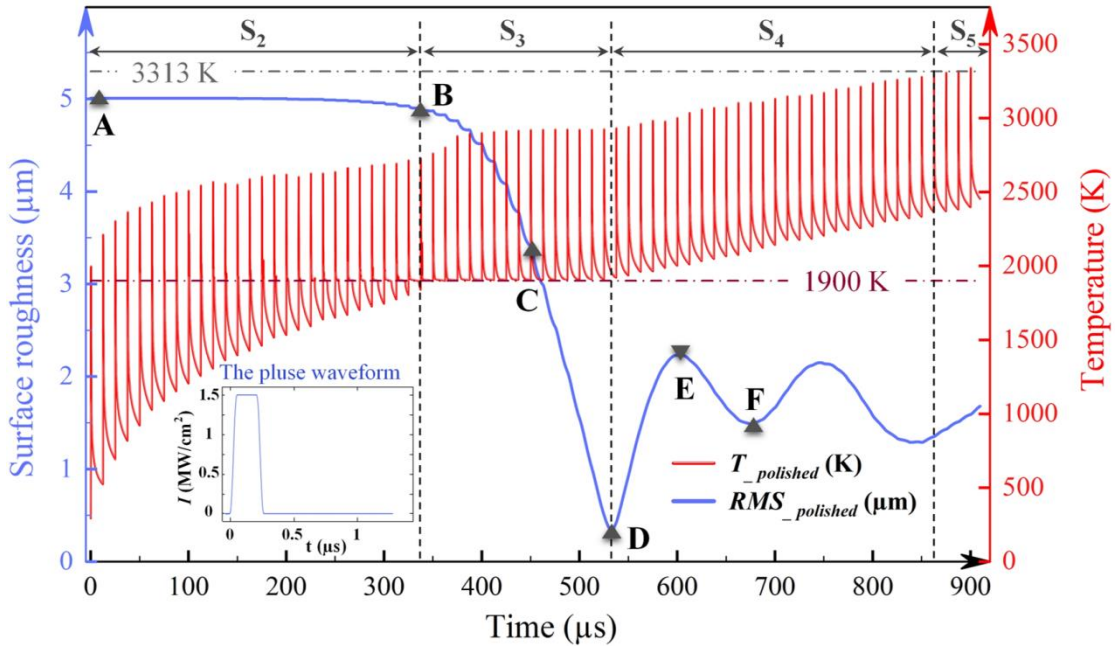

Figure s3. Temporal evolution of surface roughness versus temperature for pulsed laser polishing of Ti6Al4V materials [7]

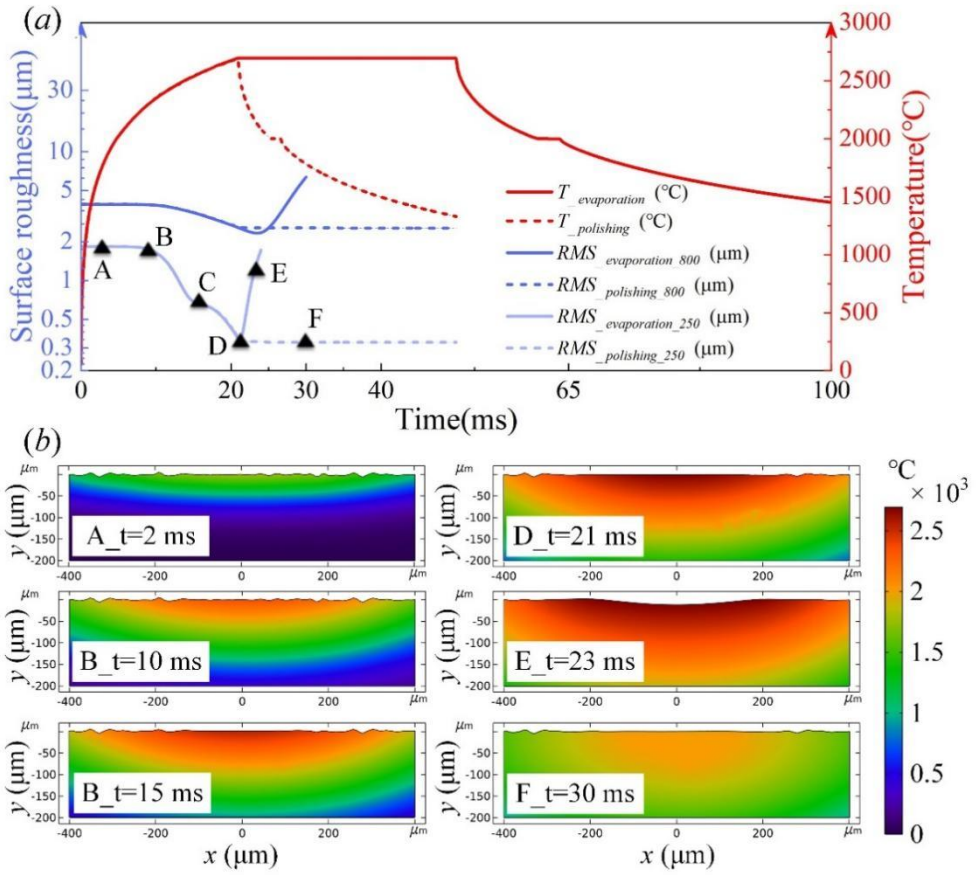

Figure s4. Temporal evolution of the surface roughness of quasi-continuous CO_2 laser action on fused silica, (a) surface roughness and temperature; (b) molten pool and surface topography.

As can be seen from figures s3 and s4, the polishing time scales are on the order of microseconds for metals and milliseconds for glass.

S4 Experimental setup

The Fig.s5 illustrates the spatial positions of the carbon dioxide laser beam relative to the femtosecond laser beam (probe pulse), showing an approximate 15° between them.

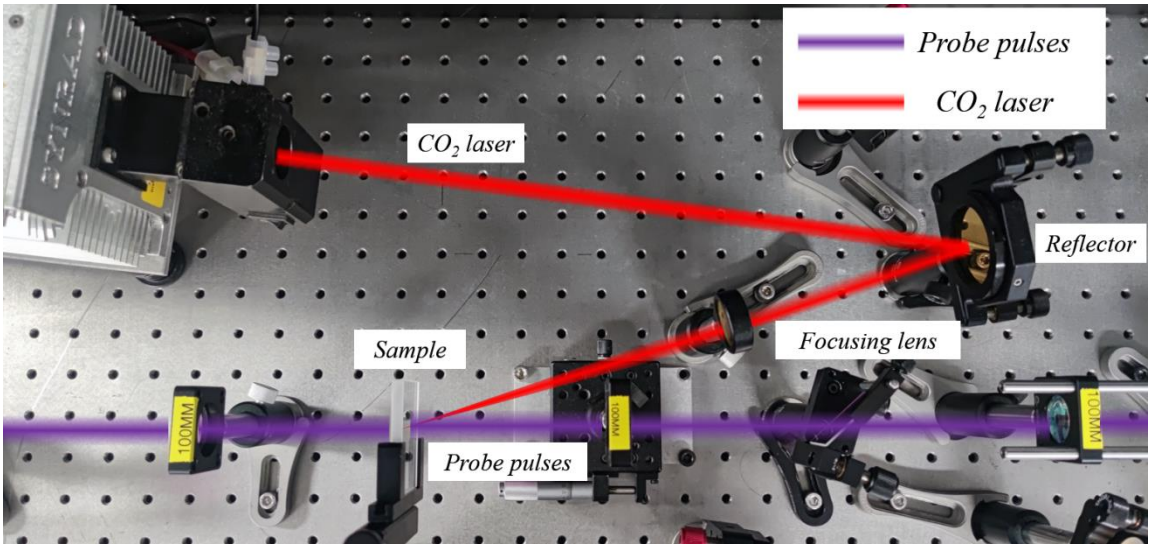

Fig s5. Spatial position of the carbon dioxide laser beam in relation to the probe pulses

S5 Experimental results-raw signal data from Fig. 3 in the manuscript

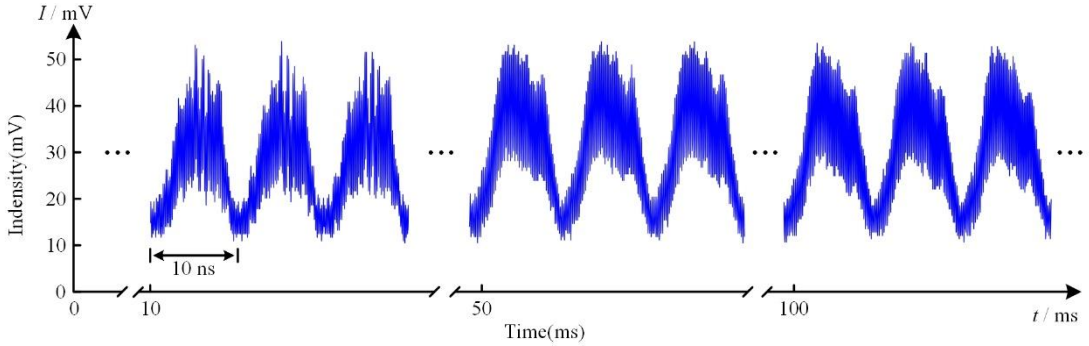

Fig.s6. The nanosecond timescale raw signal from Fig. 3 of the main manuscript

References

1. Yu, M. et al. Effects of fictive temperature on mid-frequency waviness in laser polishing of glass. *Applied Optics* **61**, 7315-7322 (2022).
2. Khairallah, S.A. et al. Controlling interdependent meso-nanosecond dynamics and defect generation in metal 3D printing. *Science* **368**, 660-665 (2020).
3. Yan, Z. et al. Numerical simulation on nanosecond laser ablation of titanium considering plasma shield and evaporation-affected surface thermocapillary convection. *Optics Communications* **453**, 124384 (2019).
4. Tan, C. et al. Experimental and theoretical investigation of localized CO2 laser interaction with fused silica during the process of surface damage mitigation. *Results in Physics* **16**, 102936 (2020).
5. Hildebrand, J. et al. Laser beam polishing of quartz glass surfaces. *Physics Procedia* **12**, 452-461 (2011).
6. Weingarten, C. et al. Laser polishing and laser shape correction of optical glass. *Journal of Laser Applications* **29**, 011702 (2017).
7. Zhao, S. et al. Analysis of molten pool dynamics and surface smoothing time scale in laser polishing alloy materials. *Optics & Laser Technology* **161**, 109183 (2023).